Numerical Simulation of Wear Phenomena

M. Chiumenti

C. Agelet de Saracibar

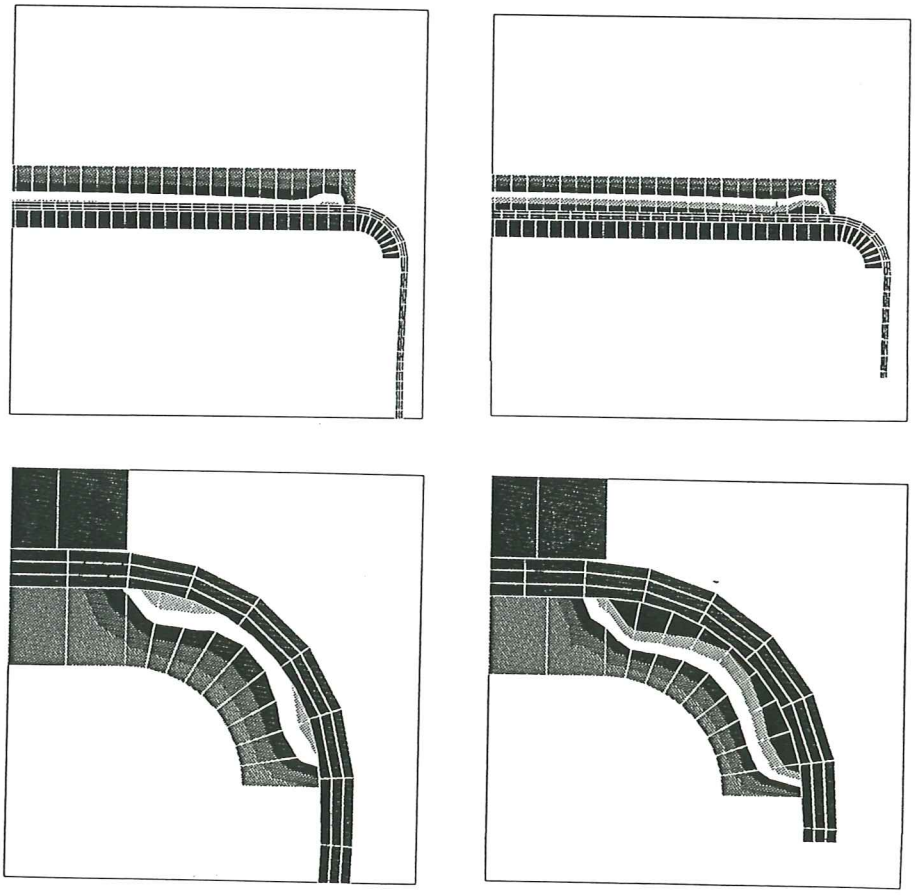

Publication CIMNE Nº 68, July 1995

Numerical Simulation of Wear Phenomena

M. Chiumenti
C. Agelet de Saracibar

Publication CIMNE Nº 68, July 1995

International Center for Numerical Methods in Engineering
Gran Capitán s/n, 08034 Barcelona, Spain

CONTENTS

1. INTRODUCTION

Over the last few years a remarkable progress has been achieved in the field of computational contact mechanics.

The formulation by means of variational inequalities, as well as the use of return mapping algorithms and tools of mathematical programming have provided efficient frameworks for the numerical treatment of such problems.

The objective is the numerical simulation of the frictional behavior of steel sheets subjected to large sliding distances and variable normal pressures.

A simple phenomenological model for frictional contact accounting for wear effects is proposed with a view to its prediction and consequent minimization.

Within the context of thermodynamics with internal variables, the coefficient of friction is assumed to be a function of the density of frictional work resulting in a theory analogous to classical work hardening elastoplasticity.

The finite element simulation of a series of sliding tests is carried out and the results are compared with experiments.

The calculation presented in the following have been performed at the ¨Centro Internacional de Metodos Numericos en Ingenieria¨ (CIMNE) in Barcelona, Spain with the program for finite element analysis FEAP.

2. NUMERICAL MODEL

2.1 Element technology

Introduction

During stamping or deep drawing operations the sheet is subjected to a very complex deformation history and a very complex boundary conditions.
For example, it is well known that some parts of the sheet deform under pure stretching, whereas other parts can develop significant bending strains. Deformation can be very complex when severe bending, or contact with tools exist.

Solid elements

Solid elements are used to simulate sheet forming where fully three dimensional theory is needed to describe deformation process.
Here a brief outline of the continuum element developed for the program is given. Detailed reference can be found in [6].

The formulation is based on the Hu-Washizu variational principle.
The finite strain elasto-plastic model used employs the multiplicative decomposition of the deformation gradient tensor F into its elastic and plastic counterparts: $F = F^e \cdot F^p$
The stresses are recovered from an hyperelastic potential written in terms of elastic Almansi strains. Plasticity is taken into account by means of the J_2 model implemented with the split operator method: elastic predictor - plastic corrector.

To avoid the volumetric locking the *B-bar method* for incompressibility is used.

The basic idea is to construct an assumed strain method in which only the dilatational part of the displacement gradient is the independent variable. The main motivation is the development of a finite element scheme that properly accounts for the incompressibility constraint emanating from the volume preserving nature of the plastic flow.

According to the preceding ideas a scalar volume-like variable $\theta \in L_2$ is introduced to consider the following assumed strain field :

$$\varepsilon = dev\left(\nabla^S u\right) + \frac{1}{3}\theta \cdot \mathbf{1}$$

where $\mathbf{1} = [1,1,1,0,0,0]$.

Similarly a pressure-like variable $p \in L_2$ is introduced so that the assumed stress field takes the form :

$$\sigma = dev\left[\nabla W\left(\varepsilon - \varepsilon^P\right)\right] + p \cdot \mathbf{1}$$

being $W\left(\varepsilon - \varepsilon^P\right)$ the stored energy function.

Consequently the variational structure (Hu-Washizu) of the assumed strain method takes the following form :

$$\Gamma_{n+1} = \left\{ u_{n+1} , \theta_{n+1} , p_{n+1} \right\}$$

that defines the weak forms :

$$\begin{cases} G(\aleph_{n+1}, \eta) = \left[\int_V \nabla^S \eta \cdot dev\left[\nabla W(\varepsilon_{n+1} - \varepsilon^p_{n+1})\right] + p \cdot div(\eta) \right] dV - \\ \qquad \int_V \rho\, b \cdot \eta\, dV - \int_{\partial V} \bar{t} \cdot \eta\, d\Gamma = 0 \\ \Lambda(\aleph_{n+1}, q) = \int_V q \cdot \left[div(u_{n+1}) - \theta_{n+1} \right] \cdot dV = 0 \\ H(\aleph_{n+1}, \phi) = \int_V \phi \cdot \left(-p_{n+1} + \frac{1}{3} tr\left[\nabla W(\varepsilon_{n+1} - \varepsilon^p_{n+1})\right] \right) \cdot dV = 0 \end{cases}$$

Where $\aleph_{n+1}$ are the state variables at time t_{n+1} .

Taking a discontinuous volume/pressure interpolations it is possible to solve the second and the third equation in the element domain disaccoupling and condensing the problem to reduce to an equation in which the only degrees of freedom are the nodal displacements. [5],[6]

2.2 Frictional contact treatment

Introduction

Contact and friction appears as a consequence of the interaction between different bodies. Such interaction is typical for sheet metal forming problems where the blank is formed by means of a punch. During the forming process the sheet interacts with the tools, adding a new source of complexity to the numerical simulation due to the non-linear nature of the boundary conditions.

Frictional contact algorithm

A new phenomenological model for frictional contact accounting for *wear effects* is proposed.

The goal is the numerical simulation of the frictional behavior of steel sheets subjected to large sliding distances and variable normal pressures.

Within the context of thermodynamics with internal variables, the friction coefficient is assumed to be a function of the density of frictional work resulting in a theory analogous to classical work hardening elastoplasticity.

A robust algorithm based on a split operator method, *elastic predictor - frictional sliding corrector,* is used for numerical integration of the frictional constitutive equations [7].

In this section we summarize the contact constrains assumed for the *penalty method,* and the frictional split operator with the frictional return mapping accounting for wear effects [1].

a) Penalty constrains :

The numerical treatment of frictional contact involves two main steps. In the first step a contact search procedure must be performed in order to detect the penetration between the contact surfaces. In the second one contact forces are evaluated.
The computational efficiency of the contact analysis is highly dependent on the efficiency of the contact search algorithm being a very expensive procedure and account for a considerable part of the execution of the whole program.

Referring to the *master-slave search algorithm* a gap-penetration function is defined for each slave node X as :

$$g_N(X,t) = -\left[\varphi_t^{(S)}(X) - \varphi_t^{(M)}\left(\overline{Y}(X,t)\right)\right] \cdot \nu$$

where:

$$\overline{Y}(X,t) = \underset{Y}{min} \left\| \varphi_t^{(S)}(X) - \varphi_t^{(M)}(Y) \right\|$$

is the *closest-point projection* of the slave node onto the master surface and ν is the unit outward normal to the master surface at the closest-point-projection.

Defining the nominal contact pressure as:

$$t_N(X,t) = t(X,t) \cdot \nu$$

it is possible to write the *normal contact constrains* as:

- *impenetrability*: $g_N(X,t) \leq 0$

- *non-adhesion*: $\begin{cases} t_N(X,t) \geq 0 & \text{if} \quad g_N(X,t) = 0 \\ t_N(X,t) = 0 & \text{if} \quad g_N(X,t) < 0 \end{cases}$

  or rather: $t_N(X,t) \cdot g_N(X,t) = 0$

- *contact persintency*: $t_N(X,t) \cdot \dot{g}_N(X,t) = 0$

that can be regularized with the Yosida regularization:

$$t_N(X,t) = \varepsilon_N \cdot \langle g_N(X,t) \rangle$$

where ε_N is the *normal penalty*.

Frictional effects are described using the *Coulomb slip function*:

$$\Phi(X,t) = \| t_T(X,t) \| - \mu \cdot t_N(X,t)$$

where μ is the friction coefficient and $t_T(X,t) = -\mathbb{P}_v[t(X,t)]$ is the frictional traction.

Defining the slip velocity as:

$$v_T(X,t) = \gamma \cdot \frac{\partial \Phi}{\partial t_T}$$

the resulting *frictional constrains* are:

- *admissible traction space* : $\Phi(X,t) \le 0$
- *slip rule*:

$$\begin{cases} v_T(X,t) = 0 & \text{if} \quad \Phi(X,t) \le 0 \\ v_T(X,t) = \gamma \cdot \frac{\partial \Phi}{\partial t_T} & \text{if} \quad \Phi(X,t) = 0 \end{cases}$$

  or rather: $v_T = \gamma \cdot \frac{\partial \Phi}{\partial t_T}$ *and* $\gamma \cdot \Phi(X,t) = 0$

- *slip consistency*: $\gamma \cdot \dot{\Phi}(X,t) = 0$

and are regularized introducing the *tangential penalty* ε_T as:

$$v_T(X,t) = \frac{1}{\varepsilon_T} \cdot L_{v_T} t_T(X,t) + \gamma \cdot \frac{\partial \Phi}{\partial t_T}$$

where $L_{v_T} t_T(X,t)$ is the Lie derivative of the frictional tangent traction along the flow induced by the relative slip velocity v_T [..].

a) Frictional return-mapping :

To account for wear effects is proposed an algorithm in which μ is not a constant parameter but is a function of an internal variable α, so that:

$$\mu = \mu(\alpha)$$

For the internal variable α is assumed the following evolution law :

$$\dot{\alpha} = \gamma \cdot \left[(1-\omega) + \omega \cdot \| t_T \| \right] \rightarrow \begin{cases} \dot{\alpha} = \gamma & if \quad \omega = 0 \\ \dot{\alpha} = \gamma \cdot \| t_T \| & if \quad \omega = 1 \end{cases}$$

Defining g_T as the tangential slip of the closest point projection, the resulting constrained incremental algebric problem is :

$$\begin{cases} t_{T\,\beta}^{n+1} = t_{T\,\beta}^{n} + \varepsilon_T \cdot \left[g_{T\,\beta} - \gamma^{n+1} \cdot \dfrac{\partial \Phi\left(t_N^{n+1}, t_T^{n+1}, \alpha^{n+1}\right)}{\partial t_T^{n+1}} \right] \\ \alpha^{n+1} = \alpha^{n} + \gamma^{n+1} \cdot \left[(1-\omega) + \omega \cdot \| t_T^{n+1} \| \right] \\ \Phi^{n+1} = \| t_T^{n+1} \| - \mu\left(\alpha^{n+1}\right) \cdot t_N^{n+1} \le 0 \\ \gamma^{n+1} \ge 0 \\ \gamma^{n+1} \cdot \Phi^{n+1} = 0 \end{cases}$$

where β is the generic component of the considered vector.

To integrate the frictional constitutive equations proposed is used a split operator method based on an elastic predictor (*trial state*) and a frictional sliding corrector.

The trial state, true when $\gamma^{n+1}=0$, take the following form:

$$\begin{cases} t_{T\beta}^{n+1\ trial} = t_{T\beta}^{n} + \varepsilon_T \cdot g_{T\beta} \\ \alpha^{n+1\ trial} = \alpha^{n} \\ \Phi^{n+1\ trial} = \left\| t_T^{n+1\ trial} \right\| - \mu\left(\alpha^{n+1\ trial}\right) \cdot t_N^{n+1} \le 0 \end{cases}$$

and consequently the frictional return-mapping (γ -form) is:

$$\begin{cases} \alpha^{n+1} = \alpha^{n+1\ trial} + \gamma^{n+1} \cdot \left[(1-\omega) + \omega \cdot \left\| t_T^{n+1\ trial} \right\| - \omega \cdot \varepsilon_T \cdot \gamma^{n+1} \right] \\ \Phi^{n+1} = \Phi^{n+1\ trial} - \varepsilon_T \cdot \gamma^{n+1} - \left[\mu\left(\alpha^{n+1}\right) - \mu\left(\alpha^{n+1\ trial}\right) \right] \cdot t_N^{n+1} = 0 \\ t_T^{n+1} = \mu\left(\alpha^{n+1}\right) \cdot t_N^{n+1} \cdot \dfrac{t_T^{n+1\ trial}}{\left\| t_T^{n+1\ trial} \right\|} \end{cases}$$

A linearization of the slip function is introduced to calculate γ^{n+1} :

$$\Phi_{(k)}^{n+1} + D\Phi_{(k)}^{n+1} \cdot \Delta\gamma_{(k)}^{n+1} = 0$$

with:

$$\begin{cases} \Phi_{(k)}^{n+1} = \Phi^{n+1\ trial} - \varepsilon_T \cdot \gamma_{(k)}^{n+1} - \left[\mu\left(\alpha_{(k)}^{n+1}\right) - \mu\left(\alpha^{n+1\ trial}\right) \right] \cdot t_N^{n+1} = 0 \\ D\Phi_{(k)}^{n+1} = -\varepsilon_T - \partial_\alpha \mu\left(\alpha_{(k)}^{n+1}\right) \cdot D\alpha_{(k)}^{n+1} \cdot t_N^{n+1} = 0 \\ \alpha_{(k)}^{n+1} = \alpha^{n+1\ trial} + \gamma_{(k)}^{n+1} \cdot \left[(1-\omega) + \omega \cdot \left\| t_T^{n+1\ trial} \right\| - \omega \cdot \varepsilon_T \cdot \gamma_{(k)}^{n+1} \right] \\ D\alpha_{(k)}^{n+1} = (1-\omega) + \omega \cdot \left\| t_T^{n+1\ trial} \right\| - 2\omega \cdot \varepsilon_T \cdot \gamma_{(k)}^{n+1} \\ \Delta\gamma_{(k)}^{n+1} = \gamma_{(k+1)}^{n+1} - \gamma_{(k)}^{n+1} \end{cases}$$

with initial value:

$$\gamma_{(0)}^{n+1} = 0$$

It is possible to find the implementation of this frictional constitutive equations in APPENDIX 1 .

2.3. Wear : phenomena and estimation

Introduction

The prediction of wear is one of the most important topic for the industries working in sheet and bulk metal forming processes.

With the development of technology, a demand has arisen for precision and accuracy of all machine parts, so the wear mechanical models must be able to be formulated in order to optimize the lifetime of metal forming tools.

In this report are described the different type of wear to understand this phenomenon and its influence, and is presented a possible numerical formulation with a view to its prediction and consequent minimization.

Wear mechanisms

A reliable description of wear in sheet metal forming can be the following [2]: when two surfaces are pressed together the real area of contact will be much smaller than the apparent one.

This is why the two surfaces are not perfectly plane, and thereby are in contact only in the tops (asperities).

During a forming operation the pressure on these asperities is so high that they plastically deform.

Another important aspect is the heat due to friction, induced when the sheet slides over the tool surface.

The result is an increase of heat on the contact spots during a very short time.

The high surface pressure combined with the heat generation produces welding in the asperities. Then they can break and with the oxidation and the plastic deformation can became so hard to scratch the tool surface.

It is generally accepted that wear phenomena can be divided into four primary and three secondary types.
The primary types are the following: *adhesive wear*, *abrasive wear*, *corrosive wear* and *fatigue wear*, while the secondary types are *fretting*, *erosion* and *cavitational wear*.

In sheet metal forming processes the dominating wear mechanisms are the adhesive and the abrasive wear.

Adhesive wear occurs when two smooth surfaces slide against each other and particles from one of the surfaces are torn off and adhere to the other surface.
These particles can later became detached as loose particles of wear, or they can return to the original surface.
Adhesive wear originates in strongly magnetic forces occurring when atoms are sufficiently close to each others. During sliding, a slight roughness on one surface comes into contact with roughness on the other, after which the separation probably occur on the old surface of contact when the contact is torn; a fragment of wear is formed.

Abrasive wear form occurs when a hard surface (or a soft surface containing hard particles) slides against a surface that is less firm and ploughs furrows in it.
The material from the furrows are wear particles which normally are loose.

Proposed wear model

Experiments with a plane strip have shown how the tendency to adhere is influenced by the *blank holder pressure* (q) and the *sliding length* (s), so that the die wear per unit of area (z) is estimated as:

$$z \propto q \cdot s \tag{1}$$

Considering a point *i* on the die surface the wear depth, z_i , at this point can be calculate as:

$$z_i = K \cdot \int \frac{q_i \cdot v_i}{H} dt \tag{2}$$

where v_i denotes the local sliding velocity at the point *i*, K is a wear constant and $H = H(T)$ is the local hardness on the die surface that is a function of the local temperature.

The basic idea of the wear calculation is to determine the normal pressure and sliding velocity during the forming cycle, and then calculate the wear distribution using equation (2) in a discrete form [2],[4]:

$$z_i = \frac{K}{H} \cdot \sum_n q_i^n \cdot v_i^n \cdot \Delta t \tag{3}$$

considering $H = const$ why the supporting finite element program used does not consider themomechanical coupled problems.

3. NUMERICAL SIMULATION

Introduction

The strategy employed in the numerical simulation relies on a displacement based *finite element method*. The solution of the discrete incremental boundary value problems is obtained by the *Newton-Raphson algorithm*.

The *line-search strategy* is used to optimize the problem of minimization even if the quadratic convergence can be affected.

As a result of the basic constitutive hypothesis the *penalty method* is used in the enforcement of the impenetrability constraints. The contact condition is monitored by checking the penetration of the slave nodes on the master surfaces.

In the wear algorithm the internal variable that is taken into account is the density of frictional work with a linear-softening curve .

3.1 Sliding Block on a rigid surface

Description of the problem

To test the possibility of the new algorithm implemented for the frictional contact problem a simulation that highlight the possibility of wear's prediction is carried out .
The simulation consists in a block that slides on a plane surface: the block is deformable while the surface is rigid.
A vertical load is applied on the block that results pressed on the surface and keeping this force constant an horizontal displacement is imposed.
The surfaces in contact are rough and the possibility of wear is taken into account so that the coefficient of friction changes during the analysis according to the wear effects.

Geometry and finite element discretization

The deformable block is 10mm wide and 5mm high and why the analysis is carried out in plane-strain conditions, a unit length in thickness direction is considered.
To discretize this block 20 elements are used: two lines of 10 elements to consider one element each millimeter.
The surface is 100mm long and discretized with 100 rigid elements (same elements density of the block).

Material

The material considered in the analysis is a steel with the following characteristics:

Young's modulus: $E = 210000\ N / mm^2$

Poisson's ratio: $\nu = 0.3$

The uniaxial stress_effective-strain curve of this material takes the following expression:

$$\sigma = 536 \cdot \left(0.0033 + \varepsilon_p\right)^{0.21} \quad [MPa]$$

The initial coefficient of friction introduced in the simulation concerning the virgin material is: $\mu = 0.1$ and it is assumed the following frictional linear-softening curve to consider the wear effects :

$$\mu(\alpha) = 0.1 - 0.666\text{E-}03 \cdot \alpha$$

where α is the density of frictional work measured in $[KN / mm]$.

Description of the analysis

The carried out simulation can be divided in two parts. First the block is pressed onto the rigid surface applying incrementally a vertical load of 200N/mm; second, the block is pulled along the surface with a prescribed horizontal displacement.

The block will move to the end of the surface keeping constant the load applied on the top.

During the analysis the reaction to the movement is measured in the node where the displacement is prescribed and the averaged frictional coefficient.

This second part of the simulation is carried out in only 10 steps.

The coefficients of penalization used for the penalty formulation of the frictional contact problem are :

normal penalty:	1.0E+11
tangential penalty:	1.0E+11

Results

The sequence of deformed mesh is shown in figure [3.1.1]: each position represent two time-steps of the simulation.

In the following are presented the reaction to move the block on the rigid surface, figure [3.1.2], and the average coefficient of friction measured during the simulation, figure [3.1.3].

It is possible to observe that the coefficient of friction decreases linearly with the displacement of the block. In fact it varies in function of the density of frictional work, but being the normal pressure constant, it can change only proportionally with the movement of the block.

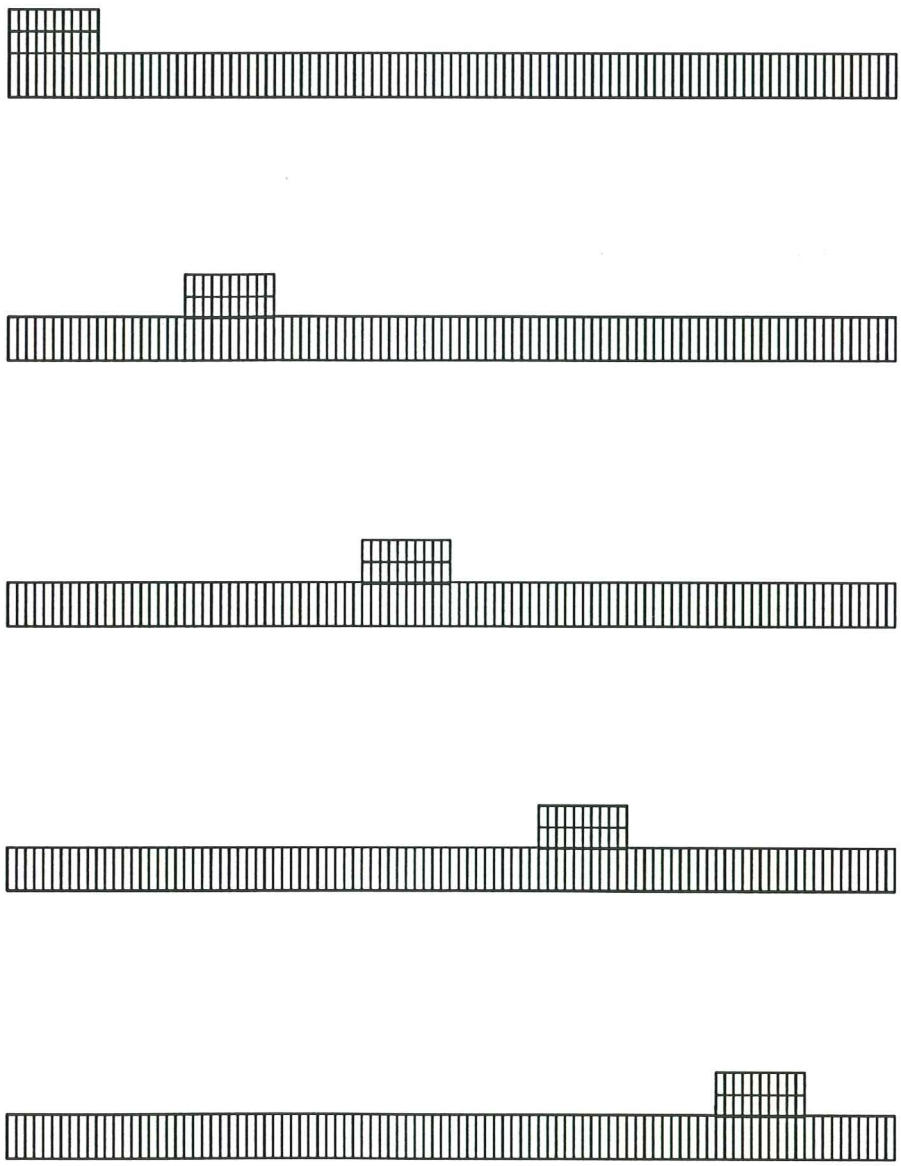

Figure 3.1.1 : Deformed mesh during the simulation

For this reason the tangential reaction must decrease with the same law as shown in the figure [3.1.2].

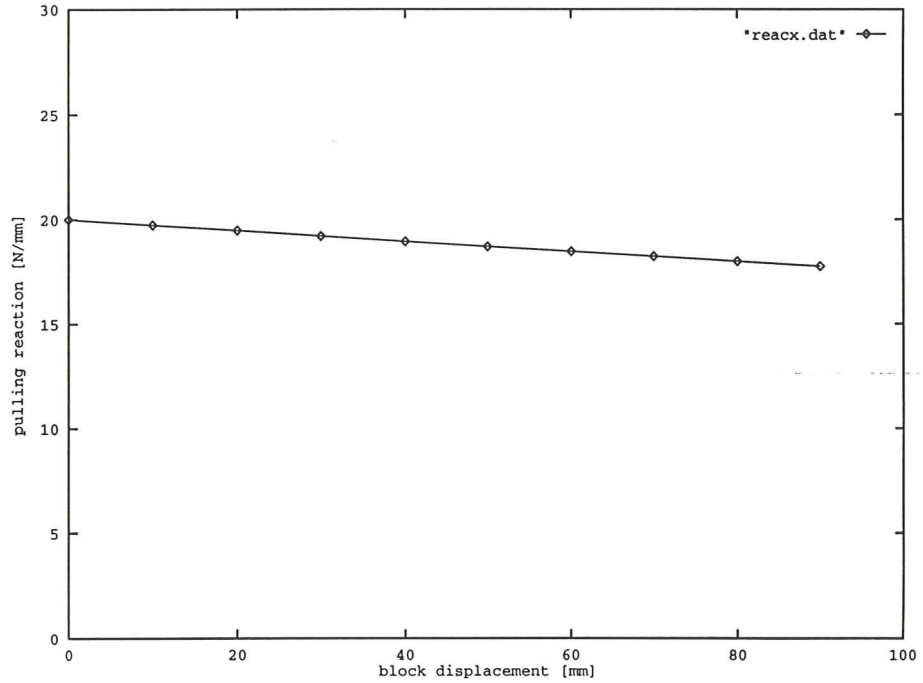

Figure 3.1.2 : The pulling reaction during the simulation

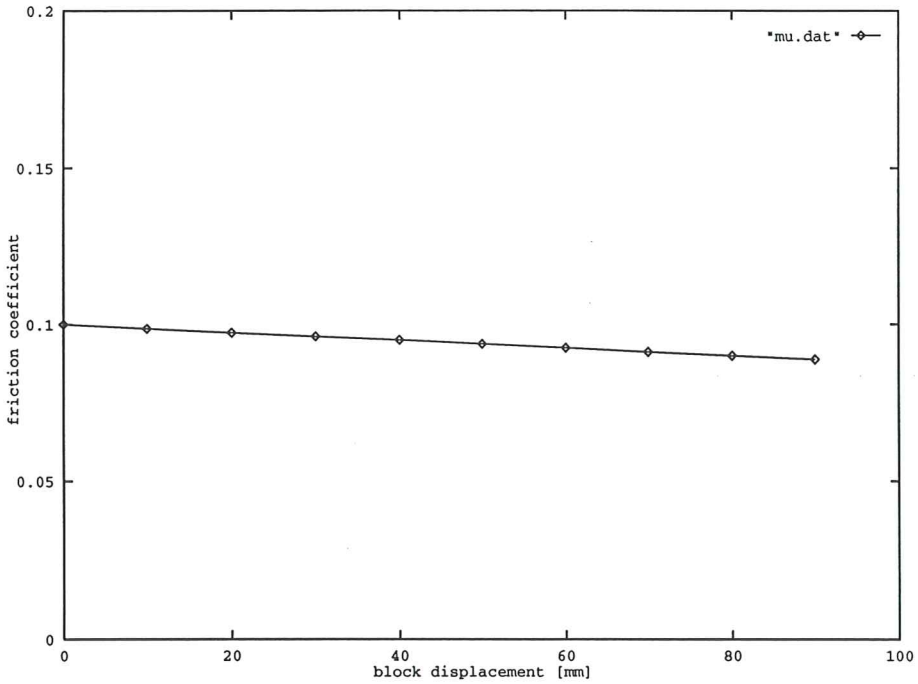

Figure 3.1.3 : Average coefficient of friction during the simulation

Figure [3.1.4] presents a typical wear map on the surface of the block (the colors does not mean anything outside the line of the surface: it is a convenient manner to represent something present only in a line).

The numerical values of the wear are given without taking into account the value of the hardness (H) and the wear constant (K):

$$\text{wear}_{\,i} = z_i \cdot \frac{H}{K} = \sum_n q_i^n \cdot v_i^n \cdot \Delta t$$

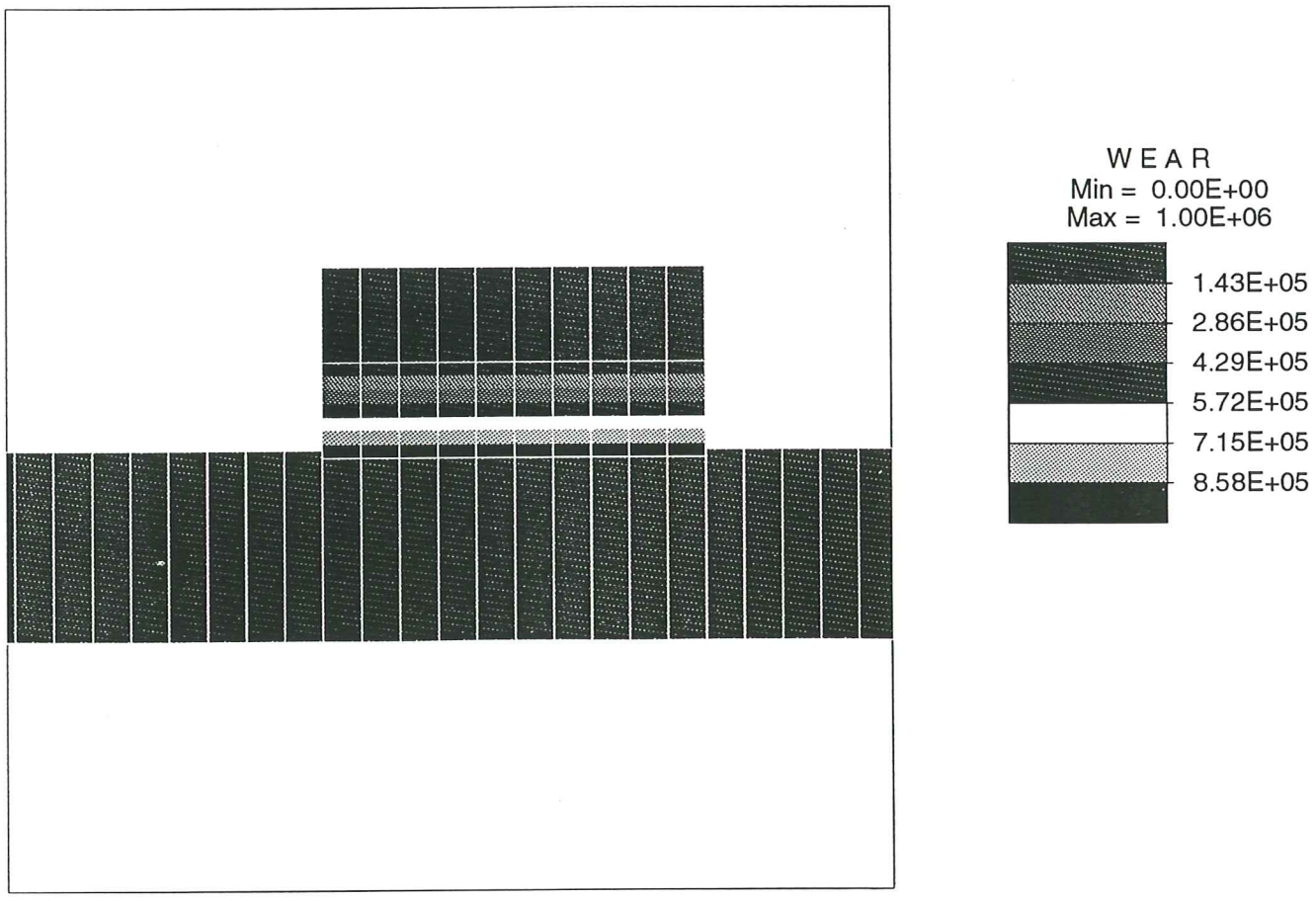

Figure 3.1.4 : Contour of Wear

3.2 Bending Under Tension (BUT) test

Description of the problem

The next analysis presented is called Bending Under Tension (BUT) test.

This analysis and the Draw Bead Simulator (DBS) test are the two test method actually used to study the wear phenomena; it is so possible to compare experimental results with the simulations.

The BUT test consists in a strip that is drawn through the dies: first through the plane section and then over the die corner, figure [a].

The strip results so pressed by the blank holder force to scrape against the plane surface of the die and then drawn over the die corner where the wear effect are measured.

All the surfaces in contact are rough and a variable frictional coefficient is taken into account.

Performing the experiments the force attributable to the friction in the plane section (F3) and the pulling force in the real analysis taking into account the bending and underbending effects (F2) are known, figure [3.2.1].

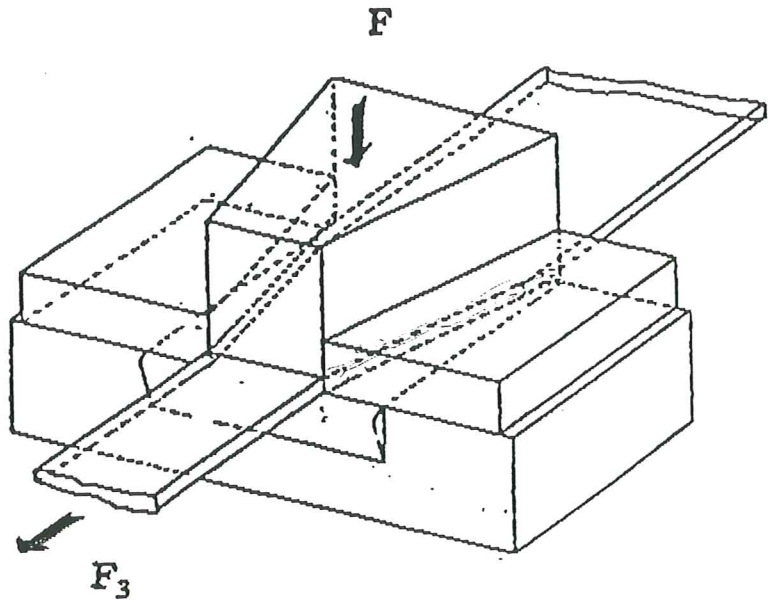

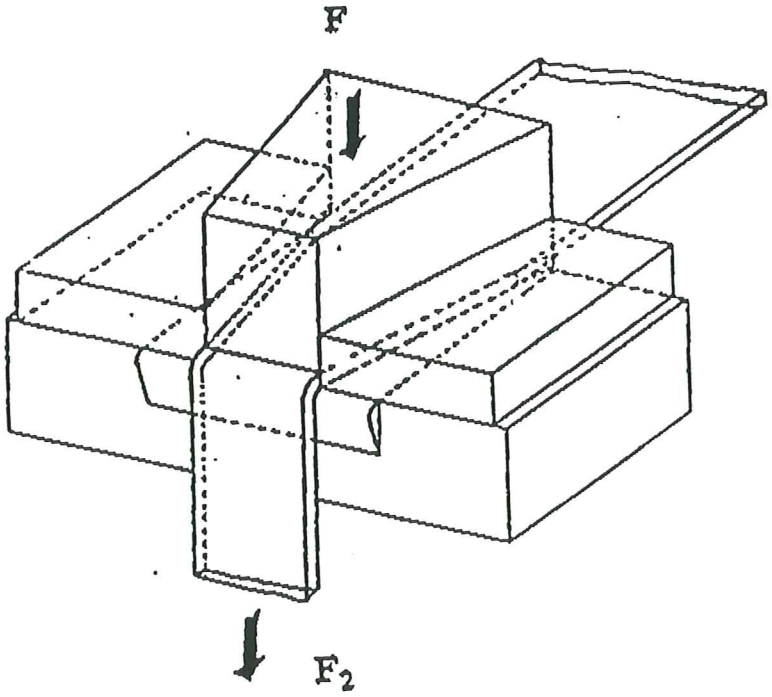

Figure 3.2.1 : Experimental test.

Geometry and finite element discretization

In the model used for the simulation the blank holder is a deformable tool and the dimensions are 125mm long, 4mm high and unit length in thickness.

It is discretized with 69 four-node elements.

The die is a rigid tool with a corner radius of 5mm that simulate the surface subjected to the highest wear effects. It discretized with 109 rigid elements.

Finally the sheet has a thickness of 1mm and is discretized with 3 lines of 109 elements each one.

The resulting total number of nodes for the mesh is 802 and the number of elements used is 507.

A high number of elements has been used for the die and the blank holder is because in the slave-master formulation of the frictional contact algorithm, the slave surfaces are the tools.

This is why the historical variable with the wear accumulated results is considered only for the slave nodes.

It results that the element size for the slave (tools) and the master (sheet) must be quite the same.

Material

The material considered in the analysis is a steel with the following characteristics:

Young's modulus: $E = 210000\ N / mm^2$

Poisson's ratio: $\nu = 0.3$

The uniaxial stress_effective-strain curve of this material takes the following expression:

$$\sigma = 536 \cdot \left(0.0033 + \varepsilon_p\right)^{0.21} \quad [MPa]$$

The initial coefficient of friction introduced in the simulation concerning the virgin material is: $\mu = 0.078$ and it is assumed the following frictional linear-softening curve to consider the wear effects :

$$\mu(\alpha) = 0.078 - 0.666\text{E-}03 \cdot \alpha$$

where α is the density of frictional work measured in $[KN / mm]$.

Description of the analysis

The analysis can be divided in two parts. First the blank holder force is applied to press the sheet against the die . Subsequently the sheet is pulled down making it slide on the die's corner .

The blank holder force is 1507.7 [N/mm] and the test is carried out for a slide length of 30mm.

During the test the blank holder pressure is kept constant and the pulling reaction is measured to be compared with the experimental results.

The simulation is done in 300 steps.

Note that the sheet is pre-curved round the die's corner and this simplification will affect the first part of the results missing the bending effect for the first elements of the sheet.

The coefficients of penalization used for the penalty formulation of the frictional contact problem are :

normal penalty:	1.0E+12
tangential penalty:	1.0E+10

It is possible to see that the value of the tangential penalty used for the analysis is lower than of the normal penalty. This is because higher value of the tangential penalty leads to a locking that does not permit the convergence of the solution. Using smaller value does not affect the solution (in terms of tangential reaction) and does not lock the convergence.

Results

Now the results of the simulation are presented.

Starting with the deformed mesh, figure [3.2.2] shows different time-steps of the analysis, precisely the situation every 100 steps.

In the following figure [3.2.3] it is possible to note how during all the simulation the penalty method permit to satisfy very well the impenetrability constrains, not permitting to the slave nodes (die) to penetrate the master surface.

The nodal reactions generated, are shown in figure [3.2.4].

The comparison with the experimental results is done looking at the pulling reaction necessary to draw the sheet in two different conditions: around the corner of the die, figure [3.2.5] calculating the force F2, and without bending the sheet to verify force F3, figure [3.2.6].

For the force F2 a value positioned between the experimental and the analytical one is found.

The analytical value is calculated using the following formula that does not consider bending effects [8]:

$$F_2 = F_{horiz.} \cdot e^{\mu\beta} = 2\mu \cdot F_{BH} \cdot e^{\mu\frac{\pi}{2}}$$

where β is the angle of contact in radians.

The force F3 takes exactly the experimental value.

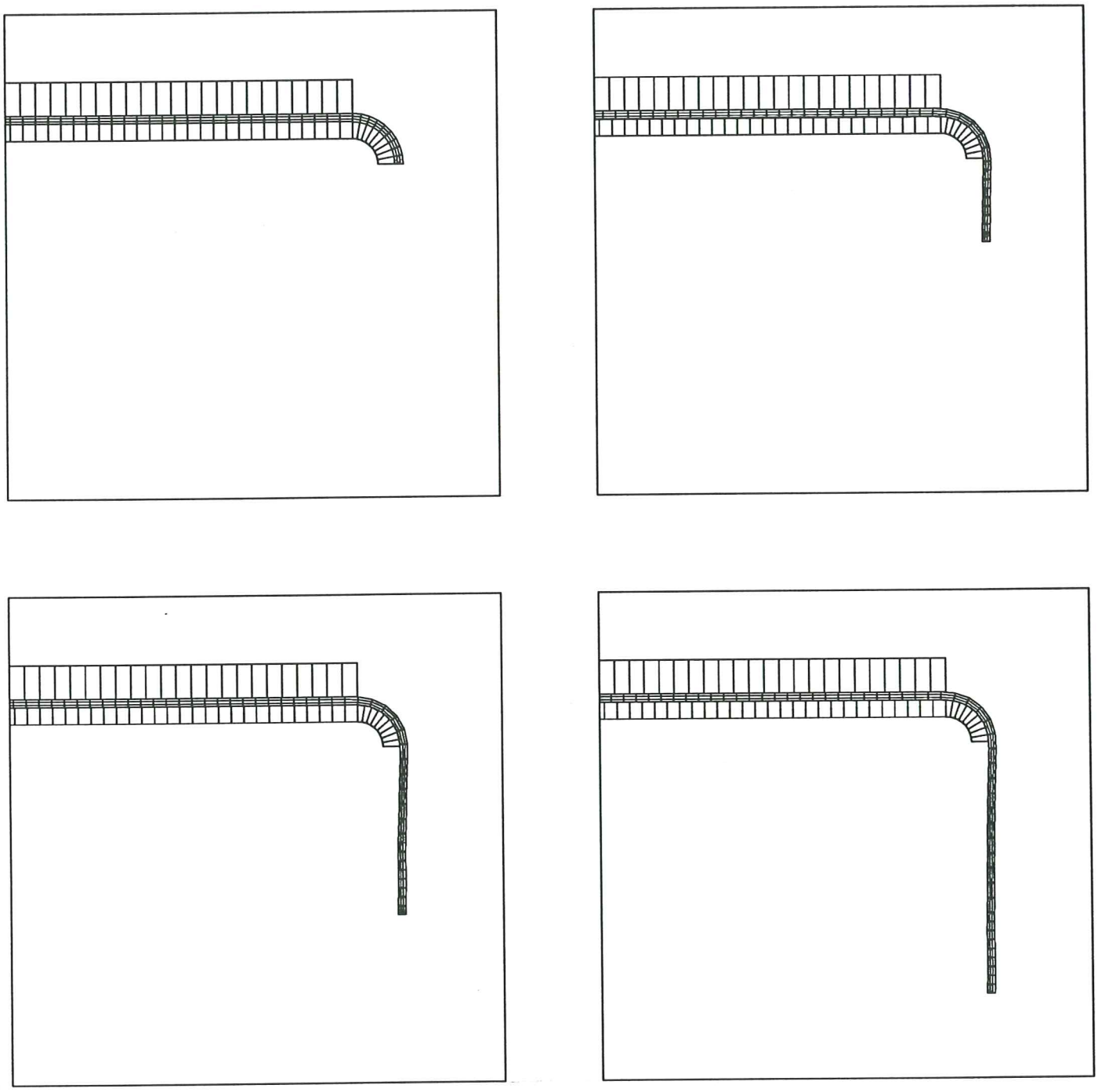

Figure 3.2.2 : Deformed mesh every 100 steps.

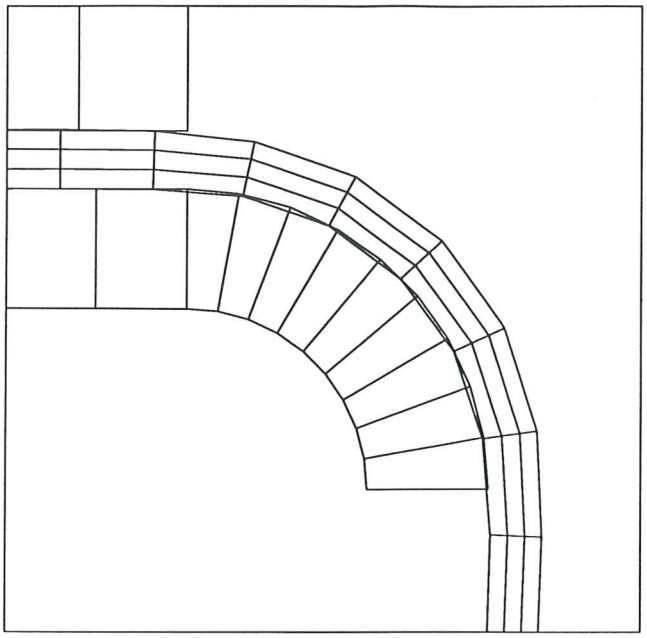

Figure 3.2.3 : Detail of the deformed mesh.

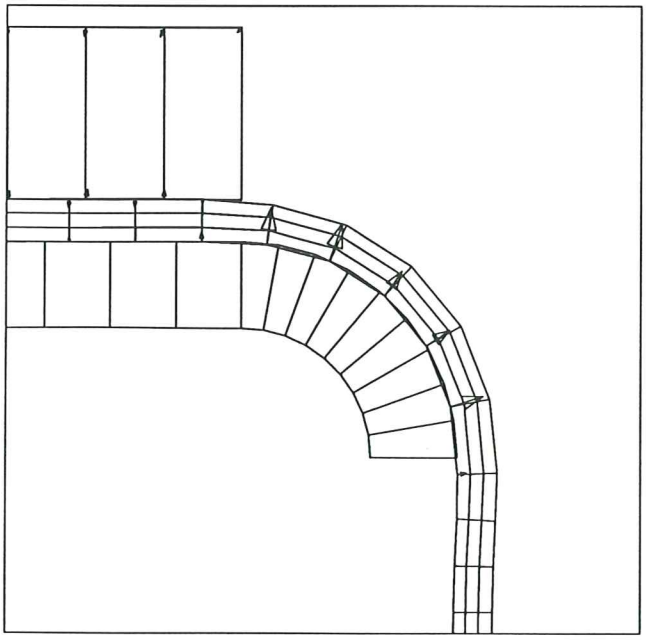

Figure 3.2.4 : Nodal reactions to satisfy the impenetrability constrains.

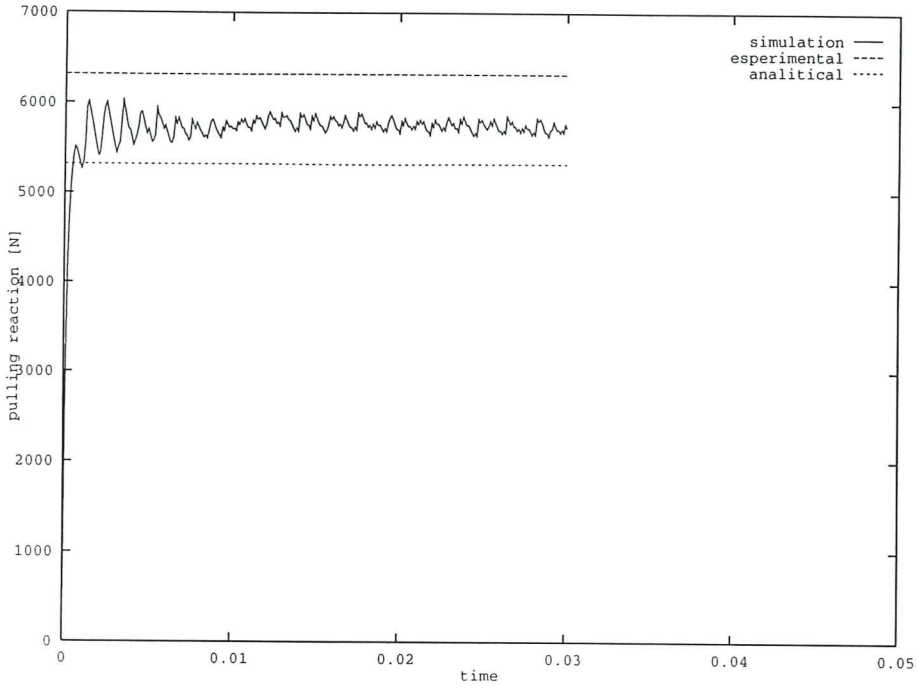

Figure 3.2.5 : Simulation of the reaction F2 : results of the simulation, value of the experiments and value of the analitical formula.

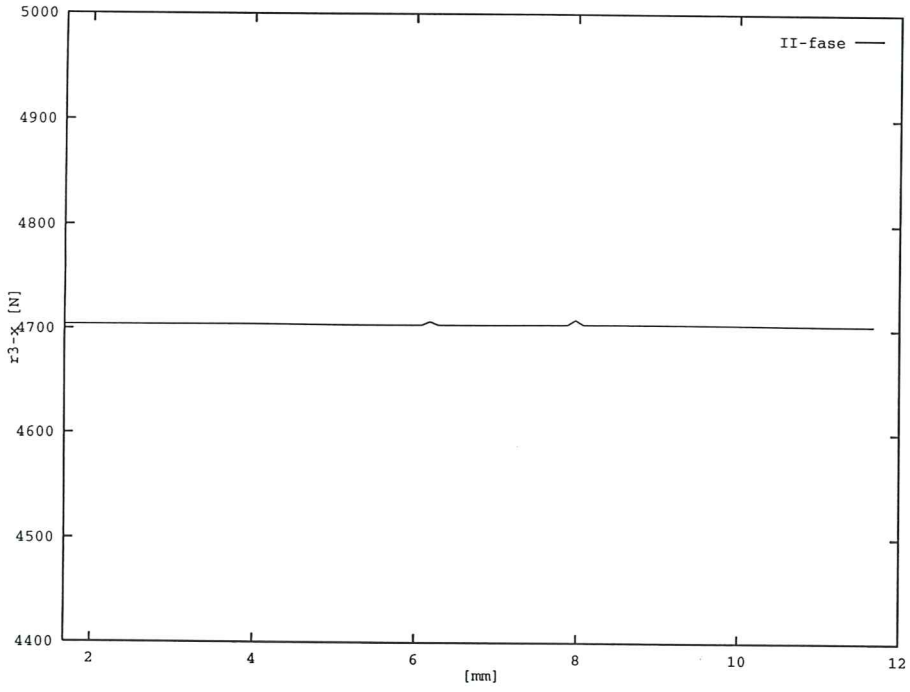

Figure 3.2.6 : Simulation of the reaction F3 concording with the experimental one.

Concerning wear results two series of contours of different time-steps are presented.

In the first one the accumulation of wear on the blank holder surface is shown in figure [3.2.7].

More interesting in the second one the same kind of contour for the die, figure [3.2.8].

In this contour is clearly possible to see the place in which the wear is accumulated, position that corresponds to the same results obteined the experimental test.

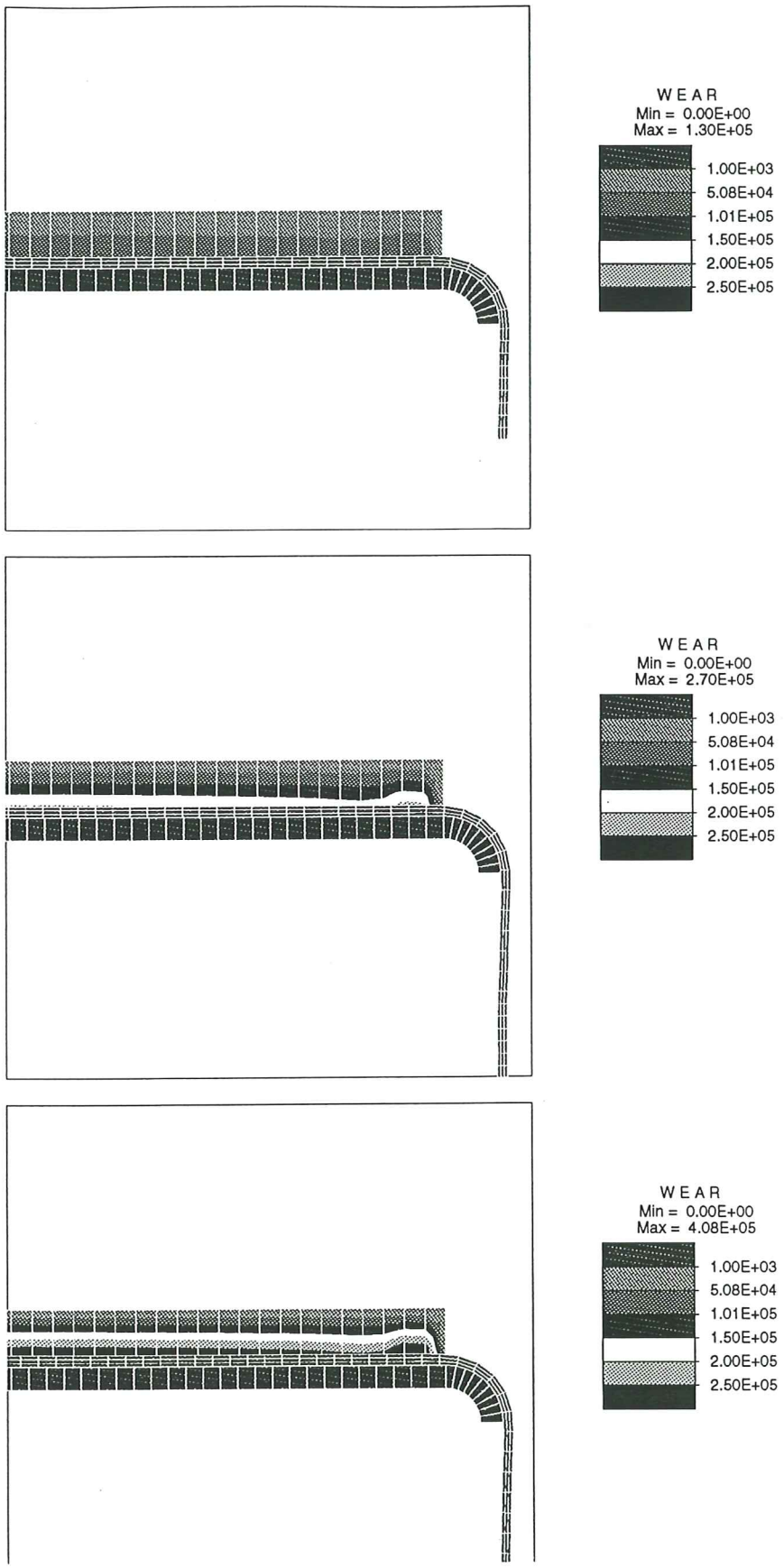

Figure 3.2.7 : Contours of the accumulated wear on the blank holder.

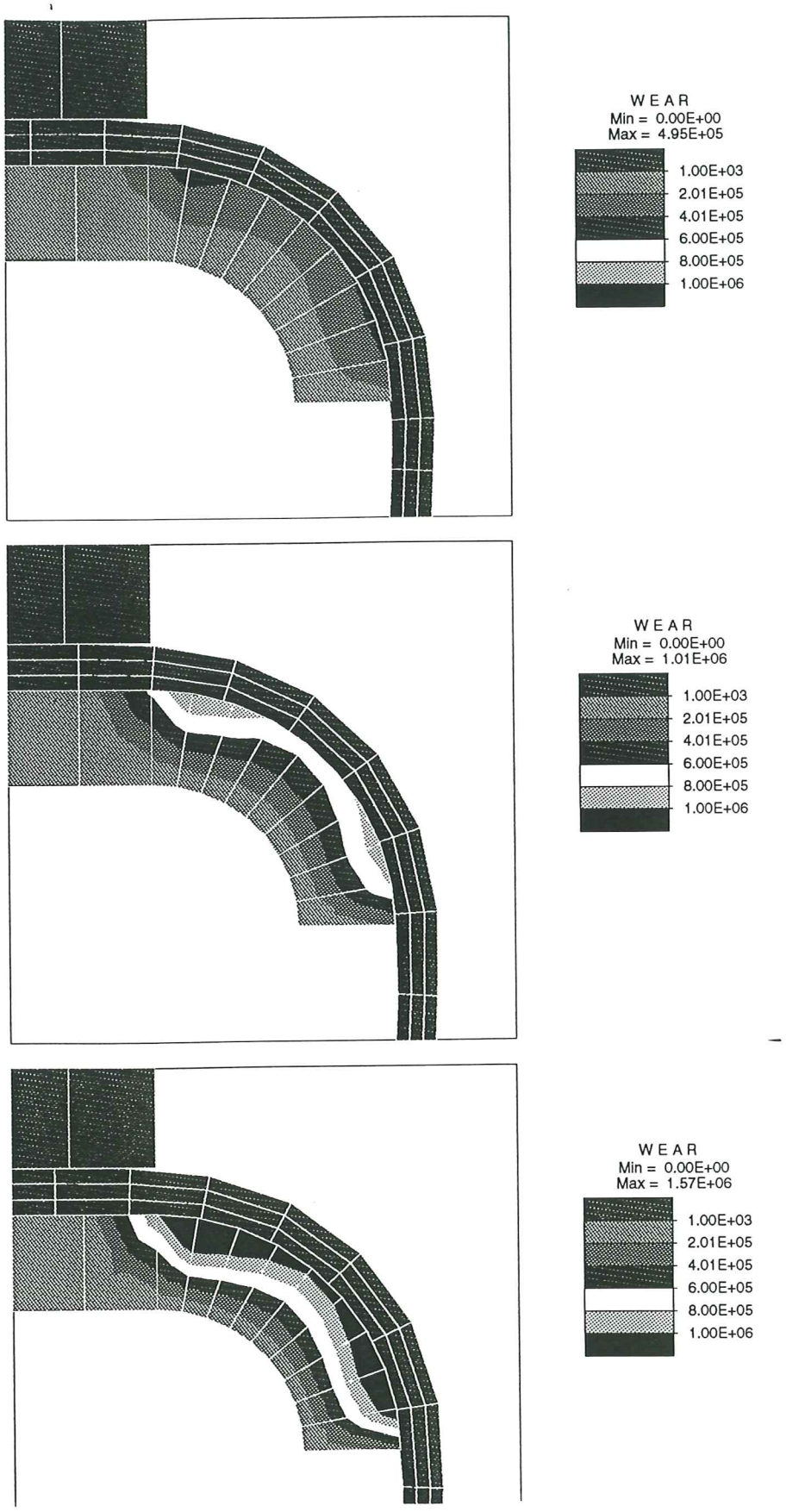

Figure 3.2.8 : Contours of the accumulated wear on the die.

3.3 Draw Bead Simulator (DBS)

Description of the problem

The Draw Bead Simulator (DBS) is the second test method used to study wear phenomena.

This test is useful to calculate the force necessary to draw a sheet through the blank holder and the die in a metal forming analysis, and is also possible to know the effects of the bead on the sheet.

The test is carried out considering a metal strip sliding through three fixed rollers that create a situation of three point bending load, figure [3.3.1]. There are two little rollers more, useful to drive the strip during the drawing simulation.

This test consist of two different phases: starting with a plane sheet the upper roller goes down bending the sheet, to simulate the bead present in the blank holder, then in the second phase the sheet is drawn out.

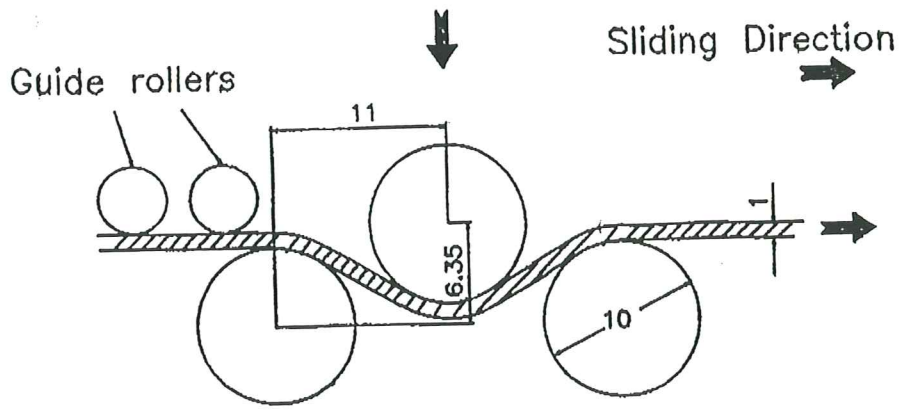

Figure 3.3.1 : The Draw Bead Simulator test (DBS)

Geometry and finite element discretization

In the simulation the blank holder is represented with the upper roller, while the die with the other two lower rollers. These rollers have a diameter of 10mm and are discretized with rigid elements.

The sheet with a thickness of 1mm is the only deformable part and is discretized with two lines and a total of 70 four-node elements .

Also for this test a plain-strain formulation is assumed, allowing to consider a 2D analysis.

Material

The material considered in the analysis is a steel with the following characteristics:

Young's modulus: $E = 210000\ N / mm^2$

Poisson's ratio: $\nu = 0.3$

The uniaxial stress_effective-strain curve of this material takes the following expression:

$$\sigma = 536 \cdot \left(0.0033 + \varepsilon_p\right)^{0.21} \quad [MPa]$$

The initial coefficient of friction introduced in the simulation concerning the virgin material is: $\mu = 0.144$ and it is assumed the following frictional linear-softening curve to consider the wear effects :

$$\mu(\alpha) = 0.144 - 0.666\text{E-}03 \cdot \alpha$$

where α is the density of frictional work measured in $[KN / mm]$.

Description of the analysis

The analysis proceed with a first part in which the upper roller moves down for 6.35mm; this part is simulated applying incrementally this displacement with 20 steps and keeping the right extreme of the sheet fixed.

Keeping now this roller fixed in this position the sheet is drawn through the three rollers pulling out to the right using a displacement control.

The analysis proceeds with 200 steps of 0.1mm to move the sheet up to distance of 20mm.

The coefficients of penalization used for the penalty formulation of the frictional contact problem are :

normal penalty:	5.0E+11
tangential penalty:	1.0E+10

Results

The results of the simulation are presented in this section, showing at first the deformed mesh in different time-steps of the analysis, precisely the situation every 50 steps figure [3.3.2].

A detail of the mesh is shown in figure [3.3.3] to check that the impenetrability constraints are well satisfied with the penalty coefficient used.

In the four following figures [3.3.4],[3.3.5],[3.3.6] and [3.3.7] a sequence of wear contour maps is presented.

Every page contains the three different tools surfaces considered for the wear analysis for different time-steps.

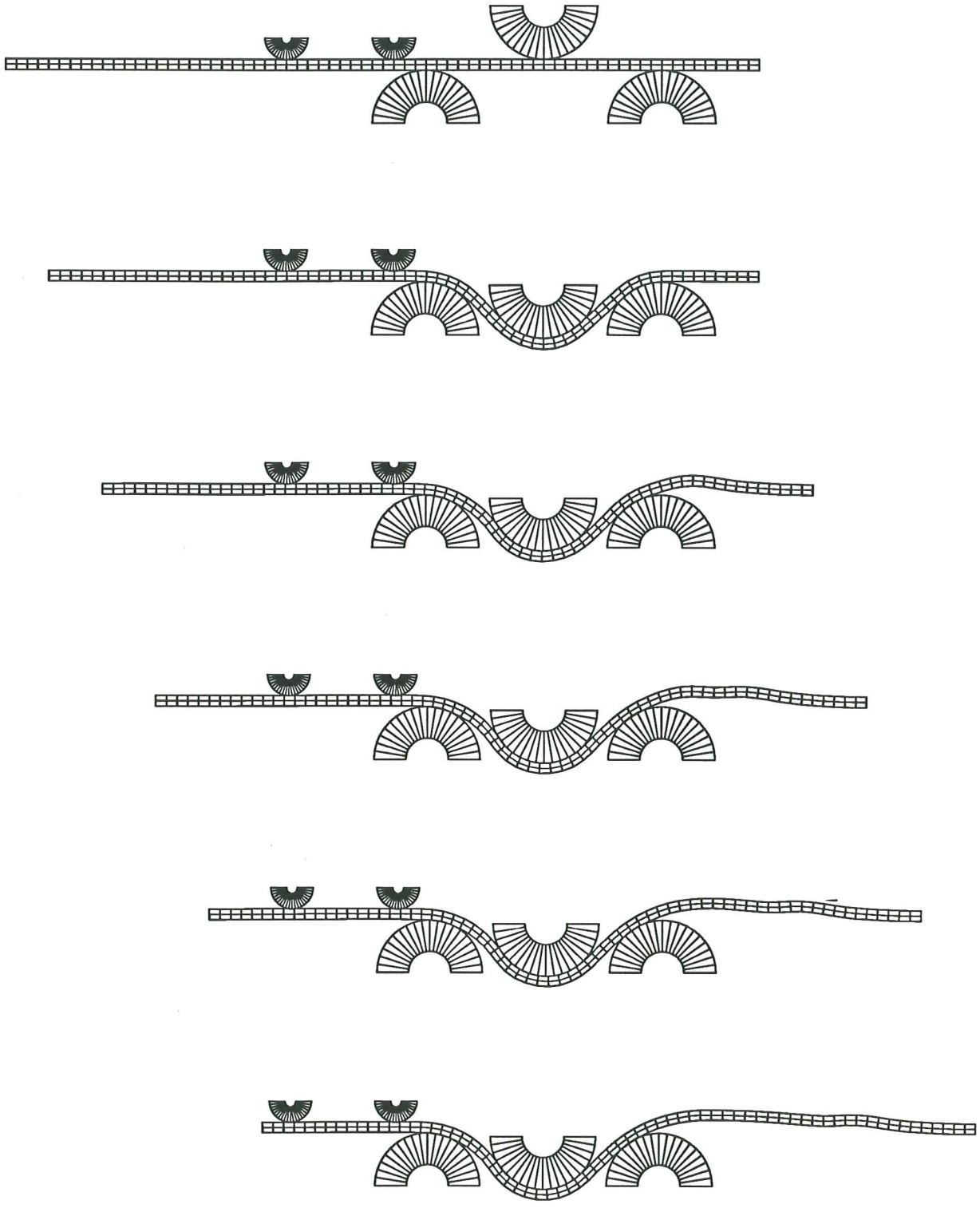

Figure 3.3.2 : Deformed mesh at different time-steps.

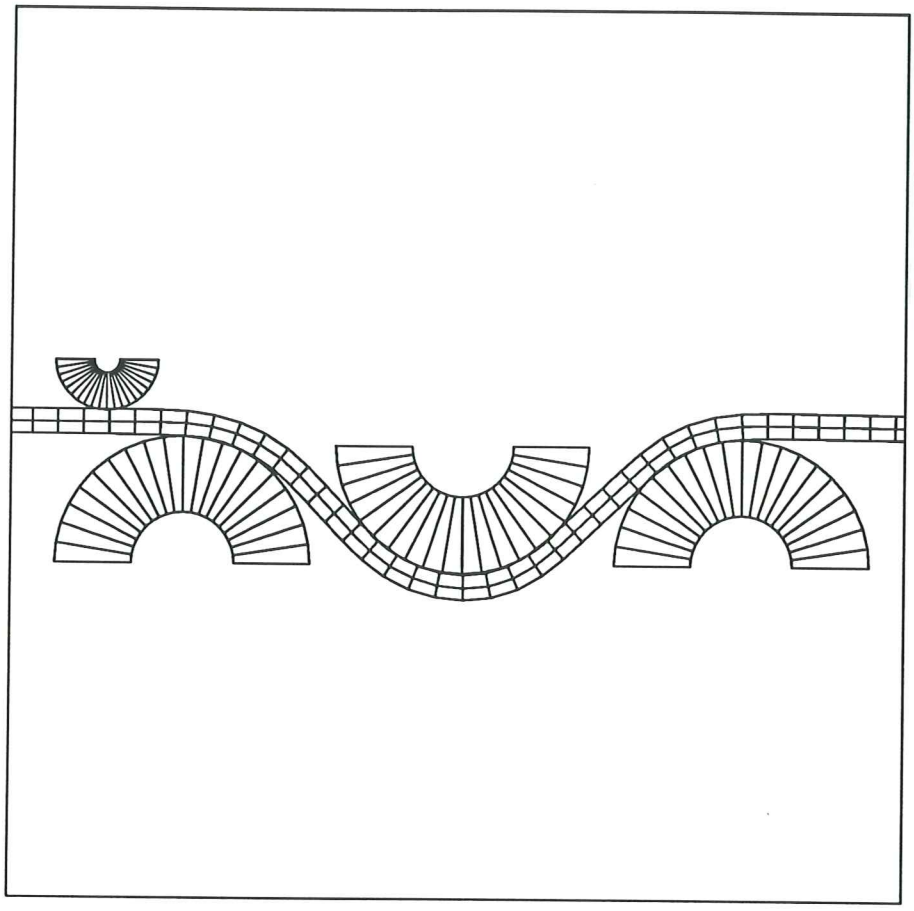

Figure 3.3.3 : Detail of the deformed mesh.

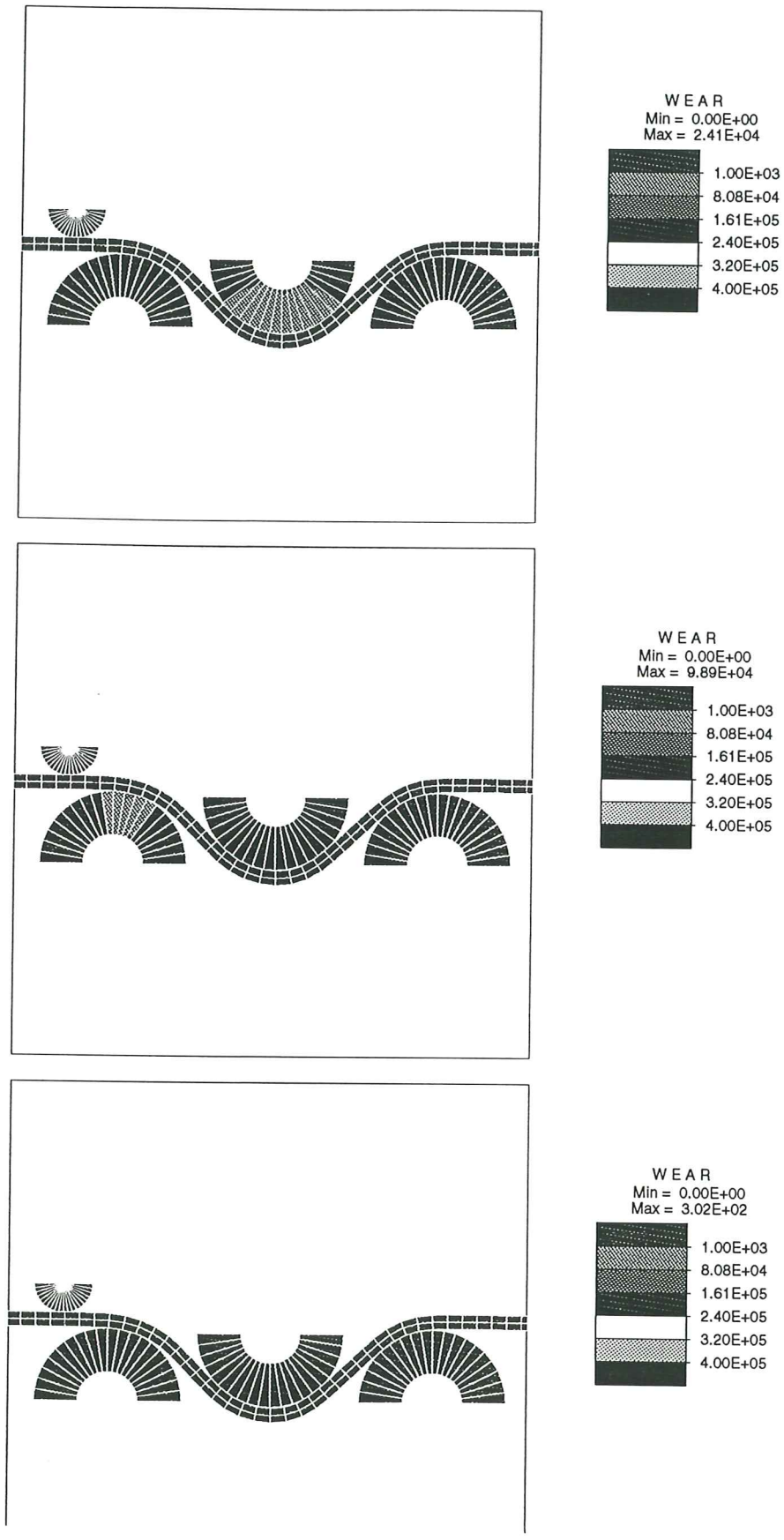

Figure 3.3.4 : Wear in the tools at the end of the first phase.

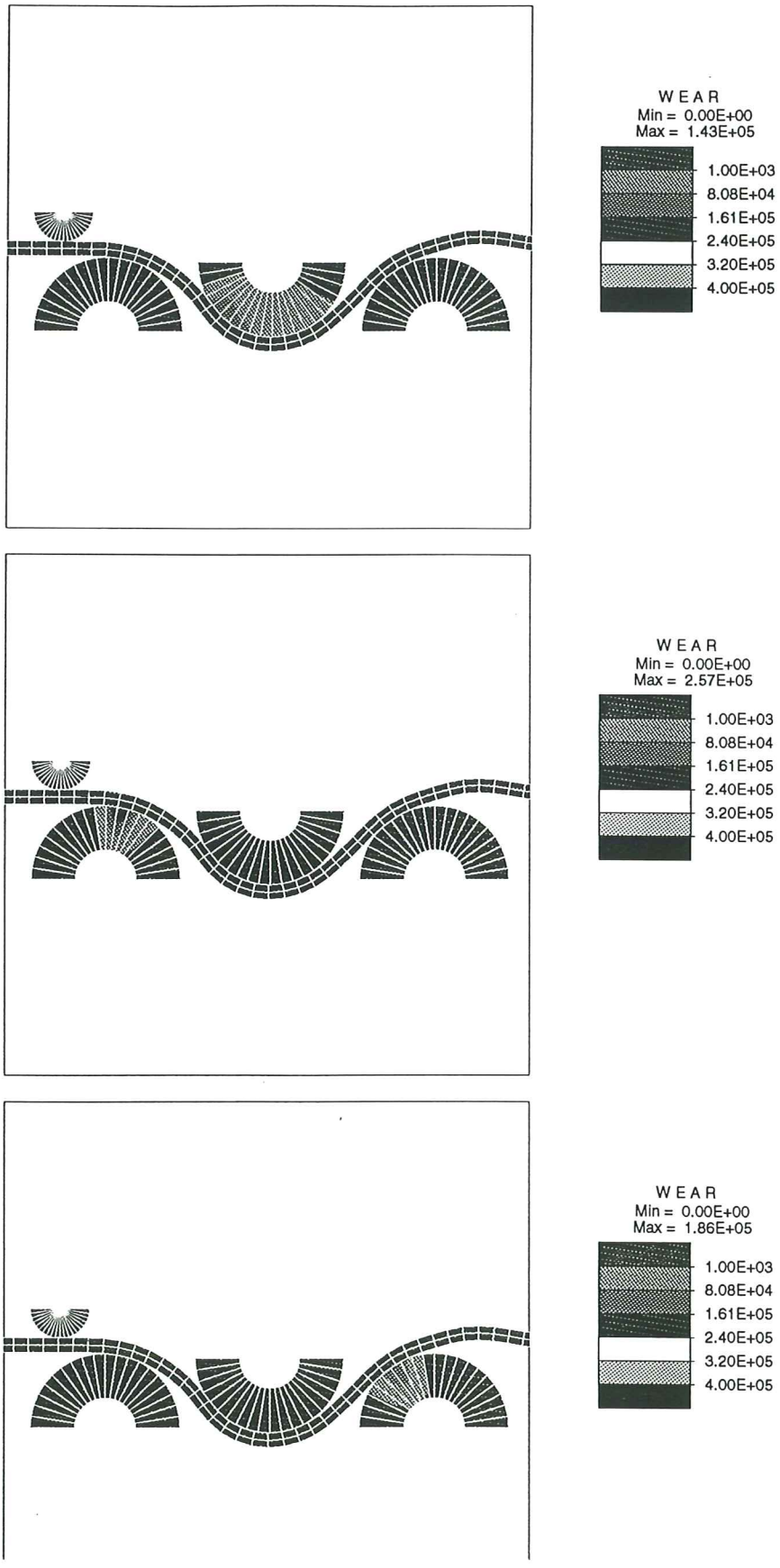

Figure 3.3.4 : Wear in the tools: time step 50.

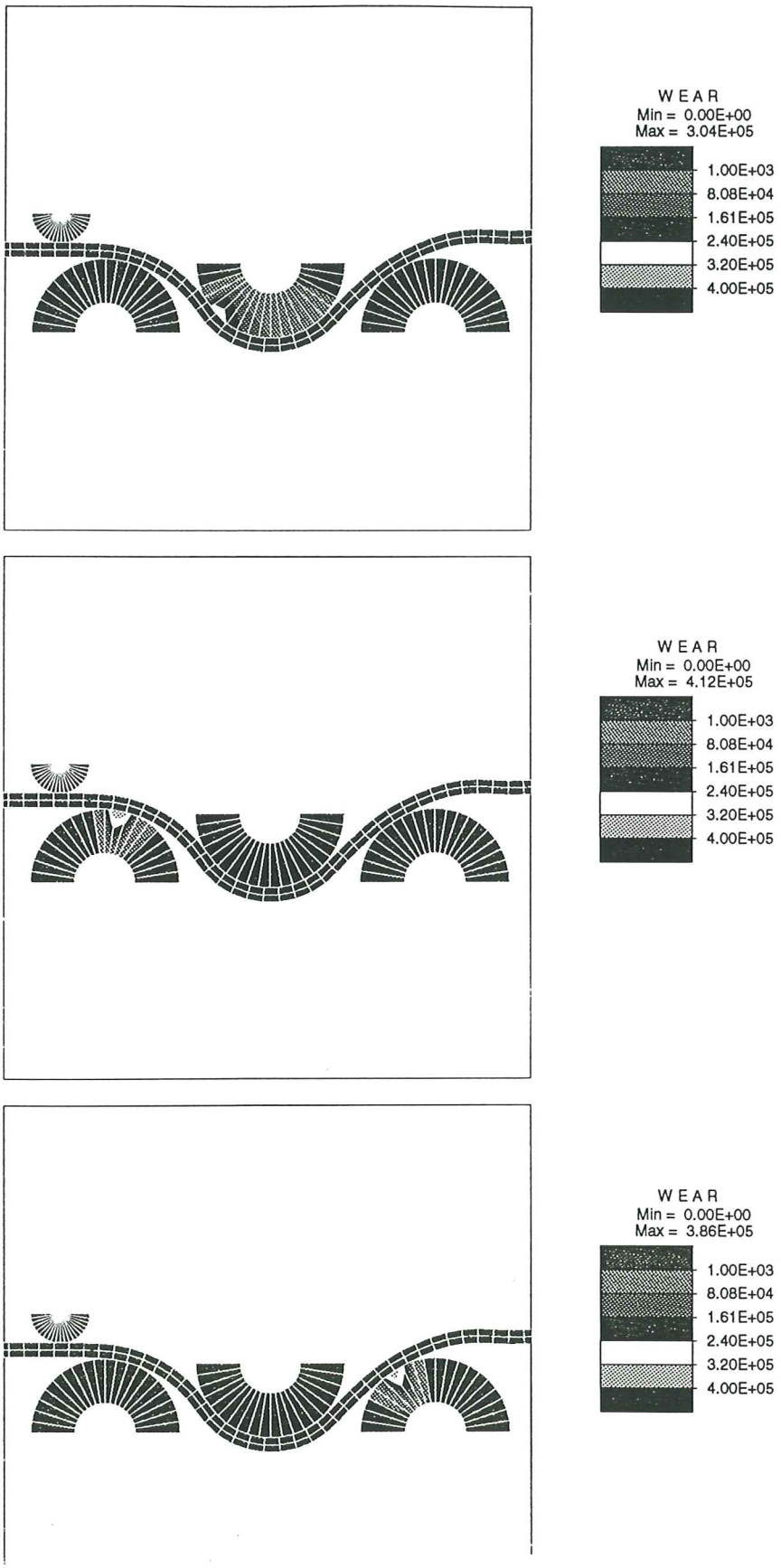

Figure 3.3.4 : Wear in the tools: time step 100.

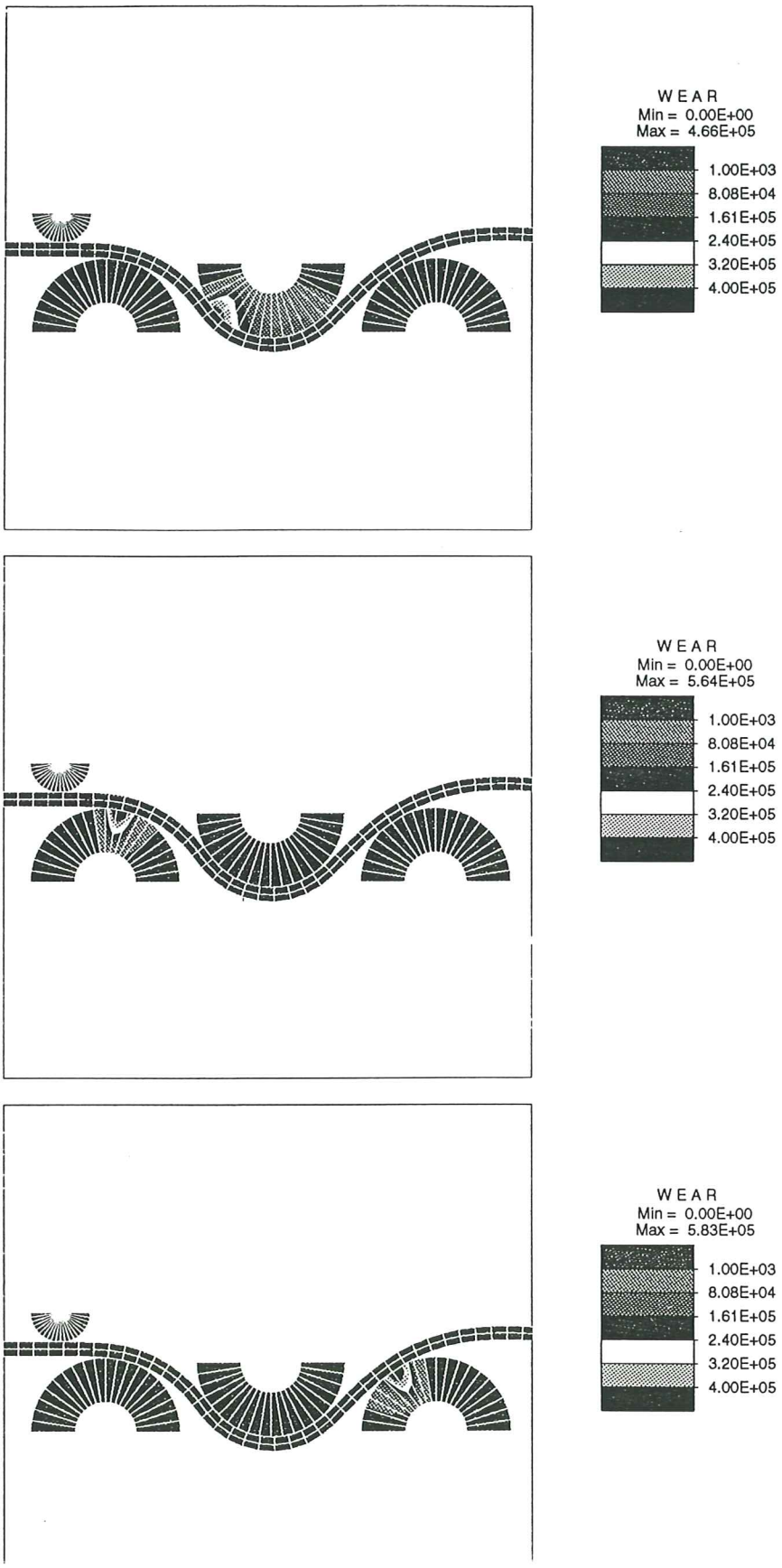

Figure 3.3.4 : Wear in the tools: time step 150.

3.4 Cutting Test

Description of the problem

In this case the algorithm of wear prediction is used to estimate the wear degradation of the tools in a cutting test.

The test consists in a sheet that lies between two cutting tools. One of these is fixed and positioned under the right side of the sheet, the other one lies onto the left side and moves down for the cutting operation.

Geometry and finite element discretization

The sheet is the only deformable part in the simulation and presents constrains in the two edges to simulate symmetry conditions.

It is 7mm long with a thickness of 0.5mm, and is discretized with 1182 four-node elements. Looking at the mesh it is possible to see high elements concentration (≈ 1000 elements) in the cutting zone that reduce in a few elements near the edges.

This is why only in this part of the sheet large deformations and high plastic stress fields are developed .

The tools are considered as rigid and present a sharp cutting edge as proposed in the expetiments. They are 3.475mm long so to leave a cutting separation of 0.05mm (10% of the thickness).

Each one of the tools is discretized with 120 rigid elements.

Material

The material considered in the analysis is a steel with the following characteristics:

Young's modulus: $E = 210000\ N / mm^2$

Poisson's ratio: $\nu = 0.3$

The uniaxial stress_effective-strain curve of this material takes the following expression:

$$\sigma = 536 \cdot \left(0.0033 + \varepsilon_p\right)^{0.21} \quad [MPa]$$

The initial coefficient of friction introduced in the simulation concerning the virgin material is: $\mu = 0.144$ and it is assumed the following frictional linear-softening curve to consider the wear effects :

$$\mu(\alpha) = 0.144 - 0.666\text{E-}03 \cdot \alpha$$

where α is the density of frictional work measured in $[KN / mm]$.

Description of the analysis

The analysis is carried out in plane-strain conditions with the displacement control of the upper cutting tool.

The other tool is completely fixed and the sheet lies on it, and presents symmetry boundary condition on the two edges.

The high number of elements that has been used for the tools is because in the slave-master formulation of the frictional contact algorithm, the slave surfaces are the tools, for the same reason discussed in the previous simulation.

This analysis will proceed for 100 steps, corresponding to the punch displacement of the 20% of the sheet thickness.

The coefficients of penalization used for the penalty formulation of the frictional contact problem are :

normal penalty:	5.0E+14
tangential penalty:	5.0E+12

Results

The results that are presented in this section refers to 100 steps of the analysis.

Figure [3.4.1] and [3.4.2] show details of the deformed mesh with its high refinement in the cutting zone, to capture as well as possible the high concentration of stresses and deformations.

To test the penetration, figure [3.4.3] shows another detail, with a zoom of the cutting tool edge. In figure [3.4.4] the reactions to satisfy the impenetrability are presented.

Contours of the equivalent-plastic-strain and plastic-ratio are shown in figure [3.4.5], and finally a detail of the wear map for the cutting tool is presented in figure [3.4.6].

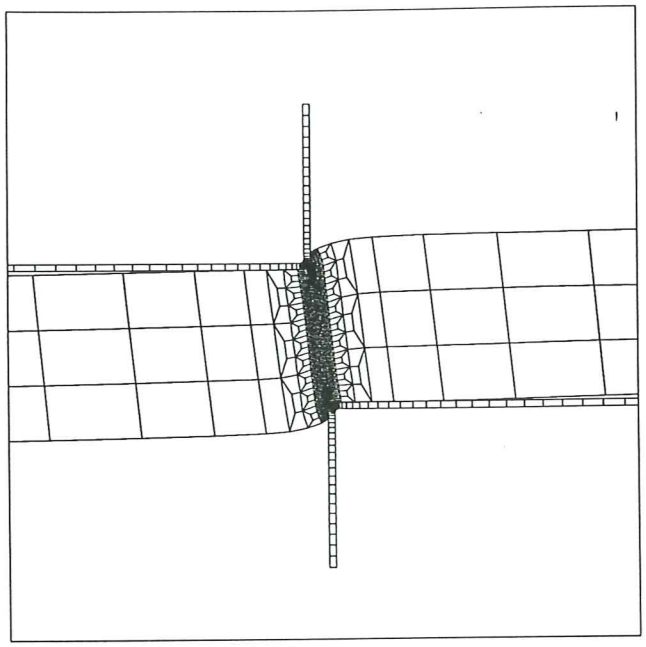

Figure 3.4.1 : Detail of the deformed mesh

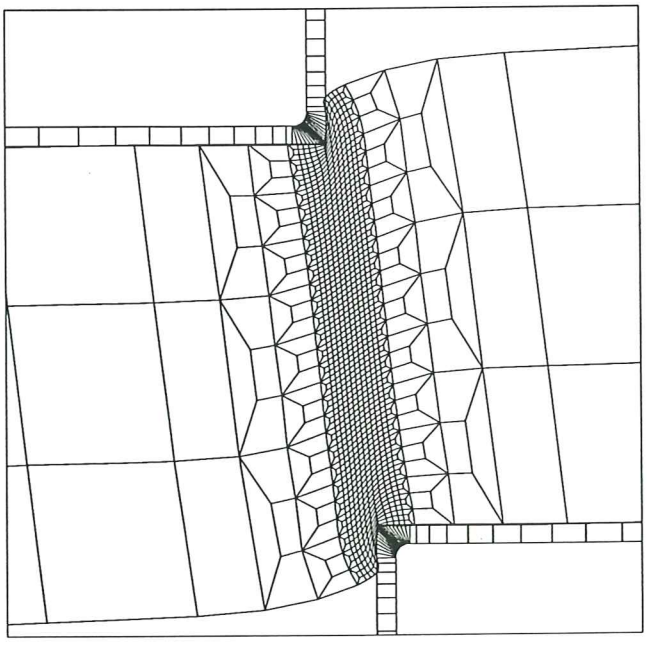

Figure 3.4.2 : Another detail of the deformed mesh

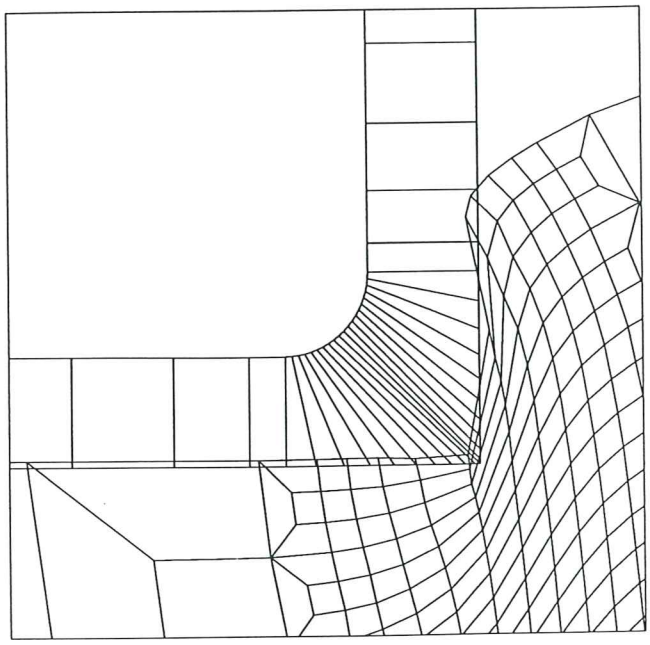

Figure 3.4.3 : Zoom to test the impenetrability constrains.

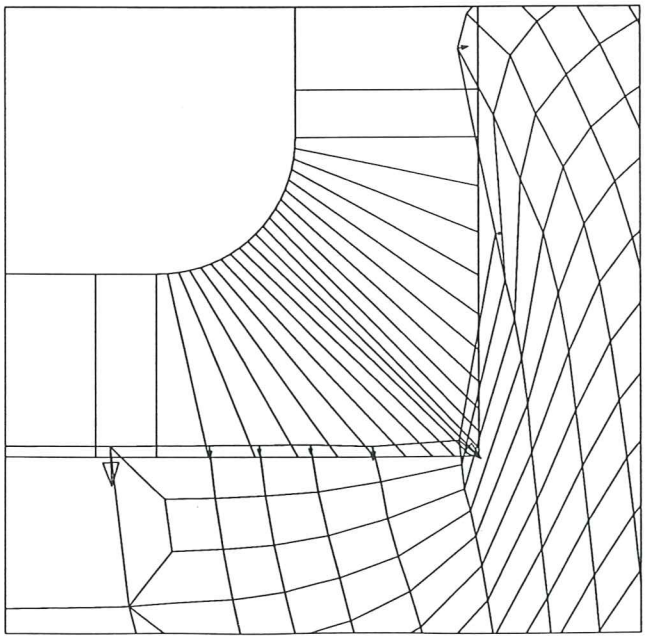

Figure 3.4.4 : Reaction to satisfy the impenetrability constrains.

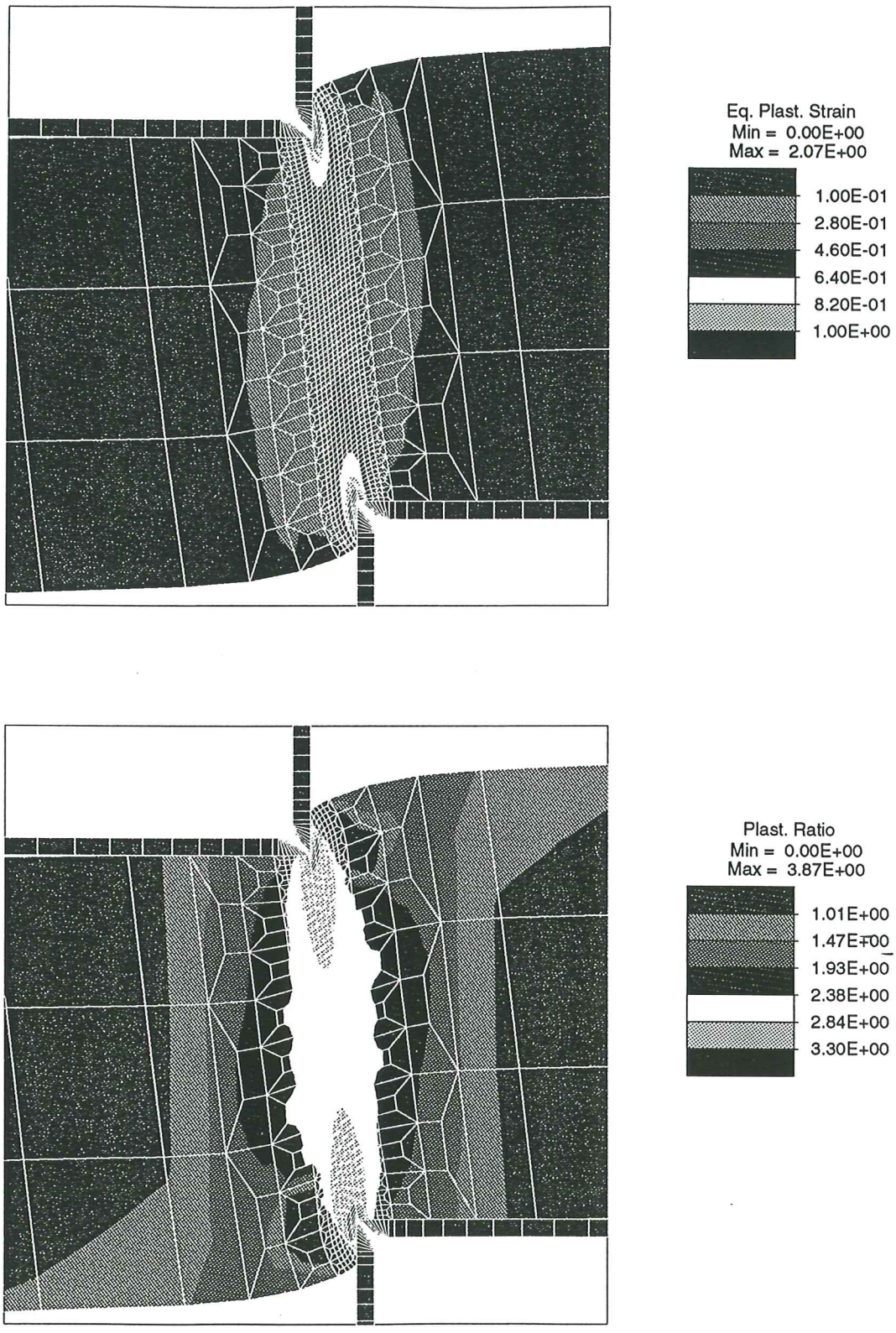

Figure 3.4.4, 3.4.5 : Contour plots of the equivalent plastic strain and plastic ratio.

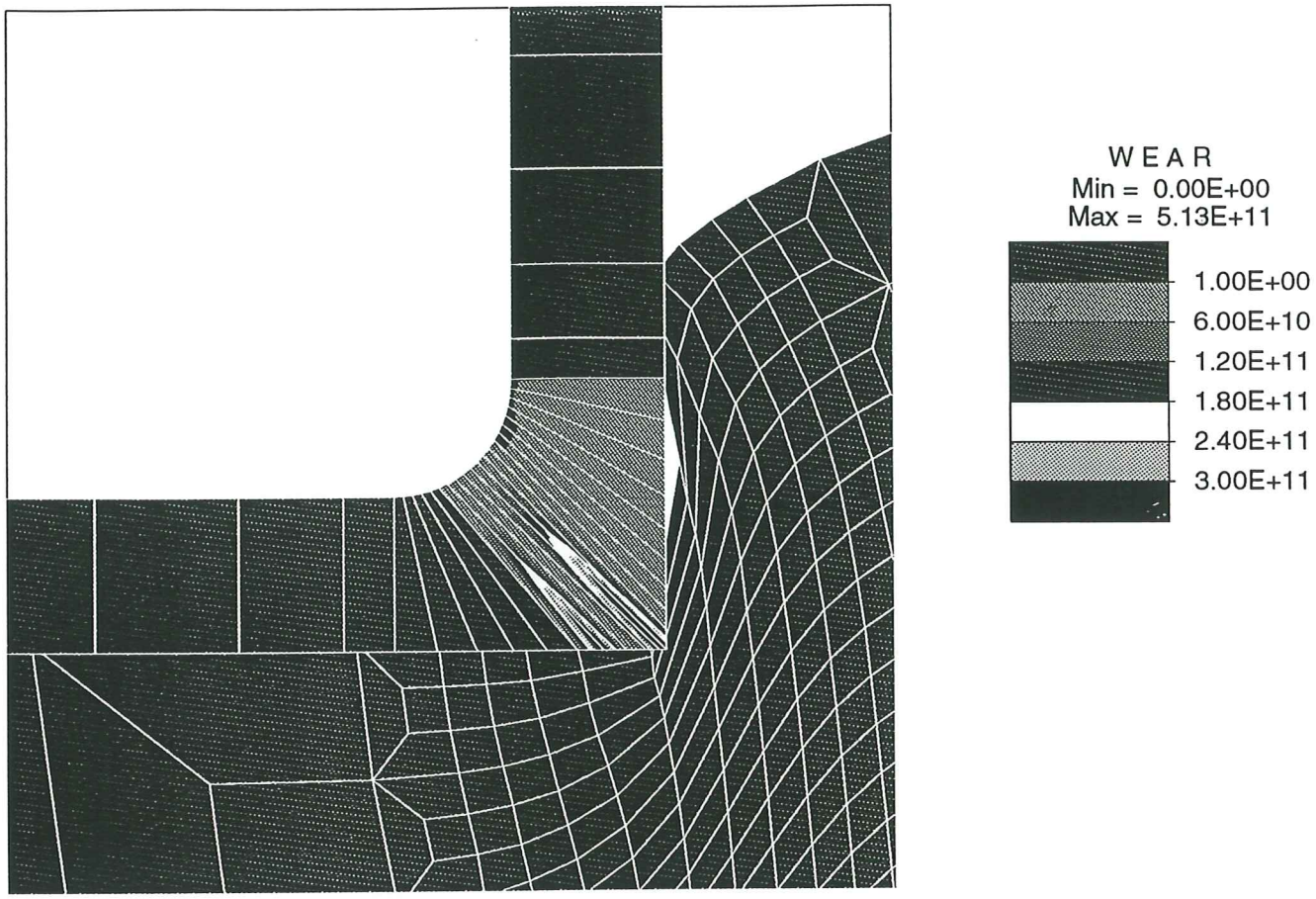

Figure 3.4.6 : Wear contour plot.

4. CONCLUDING REMARKS

A simple phenomenological model for frictional contact accounting for wear effects was presented. By adopting the frictional work as the internal variable associated to the state of the contacting surfaces, a model analogous to the classical work hardening elastoplasticity was obtained.

Numerous examples were presented with a good agreement with the experimental results, confirming that the adoption of the density of frictional work as the internal variable associated with the variation of the friction coefficient has captured the essential features of the frictional behavior of these materials when subjected to large sliding distances.

About wear prediction it is possible to see that the results were qualitatively good even if it could be interesting to verify the temperature influence in the analysis. In fact the hardness coefficient, considered in these simulations as a constant parameter, is a function of the temperature due to the heat generated in the frictional contact process.

REFERENCES

[1] C. Agelet de Saracibar, M. Chiumenti. *Numerical analysis of Frictional wear contact problems: Computational model and applications.* Preprint (1995)

[2] S. Lassen. *Formulation of wear models for forming dies.* O.P.U. (1993)

[3] T.A. Laursen, J.C. Simo. *A continuum-based finite element formulation for the implicit solution of multibody, large deformation, frictional contact problems.* International Journal Numerical Methods in Engineering, vol. 36, 3451-3485 (1993).

[4] D.R. Owen, D. Peric, A.J.L. Crook, E.A. de Souza Neto, Janguo Yu, M. Ducto. *Advanced computational strategies for 3D large scale metal forming simulation.* Proc. First Inter. Conf. Numerical Methods in Industrial Forming Processes, 18/6-21/6/1995 New York.

[5] J.C. Simo, T.J.R. Hughes. *Elastoplasticity and viscoplasticity. Computational aspects.* Preprint 1994.

[6] J.C. Simo, R.L. Taylor, K.S. Pister. *Variational and projection methods for the volume constraint in finite deformation elasto-plasticity.* Comp. Methods Appl. Mech. Eng., 51 177-208 (1985).

[7] E.A. de Souza Neto, K. Hashimoto, D. Peric, D.R.J. Owen. *A Phenomenological model for frictional contact of coated steel sheets accounting for wear effects: theory, experiments and numerical simulation.*
In Proc. 2nd Int. Conf. Numerical Simulation of 3D Sheet Metal Forming Processes, 31/8-2/9/1993, Tokyo, Japan.

[8] P. Vreede. *A finite element method for simulations of 3D sheet metal forming.* Doctoral thesis Twente University 1992, Enschede, Netherlands.

APPENDIX

In this appendix the frictional contact return-mapping algorithm implemented to study wear phenomena is presented :

SUBROUTINE contas(...)

.
.
.
.
.
.
.

```
c.....
c
c ... scelta del modello
c
c.....

      modello = 1

      if (modello .eq. 0) then
        omg = 0.0d0
      else
        omg = 1.0d0
      endif
```

```
c.....
c
c ... trial-state
c
c.....

      fortr1=pent*rmref11*gapt1+t1old


      if (icnv .eq. 0) then
       fortrnm=dsqrt(rm11u*fortr1*fortr1)
      else
       fortrnm=dsqrt(rmref11u*fortr1*fortr1)
      endif


      alfatr = rhiss(8,i)

      forn   = crds(5,i)
      ftrial = fortrnm - rmua(rmu,alfatr)*forn

c.....
c
c ... return_mapping
c
c.....

      if (ftrial .le. 0.0 .or. icds(7,i) .eq. 1) then     ! STICK
       fort1     = fortr1
       gamma     = 0.0
       alfa      = alfatr
       crds(8,i) = fort1
       rhiss(10,i) = alfa
       icds(7,i) = 1
      else                                    ! SLIP
       call gamma_form
     &      (ftrial,alfatr,forn,fortrnm,omg,pent,rmu,gamma,alfa)


       formax    = rmua(rmu,alfa)*forn
       fort1     = formax*fortr1/fortrnm
       crds(8,i) = fort1
       rhiss(10,i) = alfa
       icds(7,i) = -1
      endif
```

```
c.....
c
c ... calcolo wear_accumulato
c
c.....

      rhiss(11,i)= rhiss(9,i) + gamma*forn              ! wear-accum.



c.....
c
c ... calcolo coeff. matrice tangente
c
c.....

      if (icds(7,i).lt. 0) then                         ! if SLIP then

      dadg   = 1.0d0-omg+omg*rmua(rmu,alfa)*forn-omg*pent*gamma

      beta1  = (dadg+omg*pent*gamma)/(pent+dadg*drmua(alfa)*forn)
      beta2  = dadg/(pent+dadg*drmua(alfa)*forn)

      beta1b = beta1*drmua(alfa)*forn
      beta2b = beta2*drmua(alfa)*forn

      pt1    = fort1/dsqrt(rm11u*fort1*fort1)

      crds(15,i) = -(1.d0-beta2b)*rmua(rmu,alfa)*penn*pt1
      crds(16,i) =  beta1b*rmref11*pent
      crds(17,i) = -(rmua(rmu,alfa)*forn-beta1b/fortrnm)*rm11u*pt1

      endif
```

```
c.....
c
c ... function & subroutine
c
c.....

      function rmua(mu,a)

      real*8 rmua,a,mu
      real*8 a1,a2,a3,a4,a5

      a1 = -0.666d-7
      a2 =  0.0d0
      a3 =  0.0d0
      a4 =  0.0d0
      a5 =  0.0d0


      rmua = mu + a1*a + a2*a**2 + a3*a**3 + a4*a**4 + a5*a**5

      return
      end



      function drmua(a)

      real*8 drmua,a
      real*8 a1,a2,a3,a4,a5


      a1 = -0.666d-7
      a2 =  0.0d0
      a3 =  0.0d0
      a4 =  0.0d0
      a5 =  0.0d0


      drmua = a1 + 2.0*a2*a + 3.0*a3*a**2 +
     &        4.0*a4*a**3 + 5.0*a5*a**4

      return
      end
```

```
      subroutine gamma_form
     &          (ftrial,alfatr,forn,fortrnm,omg,pent,rmu,gamma,alfa)

      real*8  ftrial,alfatr,forn,fortrnm,omg,pent,rmu,gamma,alfa
      real*8  dalfa,dgamma,fi,dfi
      real*8  tol,dgmax
      integer nmax,iter
      real*8  rmua,drmua


      tol  = 1.d-3
      nmax = 50

      gamma = 0.0d0
      dgmax = 0.0d0
      iter  = 0



  100 iter = iter + 1

      if(iter .gt. nmax) then
        write(*,*) 'NO convergence GAMMA-RETURN-MAPPING !'
        goto 200
      endif

      alfa  = alfatr+gamma*(1.0d0+omg*(fortrnm-pent*gamma-1.0d0))
      dalfa = (1.0d0-omg)+omg*fortrnm-2.0d0*omg*pent*gamma
      fi    = ftrial-pent*gamma-(rmua(rmu,alfa)-rmua(rmu,alfatr))*forn
      dfi   = -pent-drmua(alfa)*dalfa*forn

      dgamma = -fi/dfi
      gamma  = gamma + dgamma


      dgmax = max(dgmax,abs(gamma))

      if(abs(dgamma) .lt. tol*dgmax) then
        goto 200
      else
        goto 100
      endif


  200 continue

      return
      end
```